Journal of Materials Chemistry A

ROYAL SOCIETY OF CHEMISTRY

PAPER

View Article Online
View Journal | View Issue

Cite this: *J. Mater. Chem. A*, 2022, **10**, 20024

Marine waste upcycling—recovery of nylon monomers from fishing net waste using seashell waste-derived catalysts in a CO_2-mediated thermocatalytic process†

Soosan Kim,‡[a] Yong Tae Kim,[b] Lee Seul Oh,[b] Hyung Ju Kim *[b] and Jechan Lee *[c]

A lot of fishing nets have been abandoned, lost, or discarded at sea. Herein, we aimed at applying seashell waste-derived catalytic materials to a thermocatalytic process to recover a valuable commodity chemical (*e.g.*, caprolactam) from fishing net waste (FNW) made of polyamide 6. For catalyst synthesis, seashell waste was carbonized in N_2 and CO_2 environments (denoted as SSWC-N_2 and SSWC-CO_2, respectively); here, the basicity of SSWC-CO_2 was two-fold more than that of SSWC-N_2. The thermocatalytic conversion of FNW was also conducted under N_2 and CO_2 atmospheres. Using SSWC-CO_2 in the thermocatalytic conversion conducted under a CO_2 atmosphere maximized the caprolactam recovery (80 wt% of FNW feedstock, the highest yield reported to date) possibly because the base-catalyzed decomposition of polyamide 6 was enhanced by more reactive cleavage of the amide linkage in CO_2. SSWC-CO_2 was reused for at least three cycles. In conclusion, SSWC-CO_2 is a promising alternative catalyst to recover caprolactam from FNW. The findings from this study offer insights into developing a new thermocatalytic upcycling process for marine waste such as FNW and seashell waste. This aids in reducing microplastic pollution and increasing economic potential for marine waste valorization.

Received 16th March 2022
Accepted 13th July 2022

DOI: 10.1039/d2ta02060b

rsc.li/materials-a

[a]*Department of Environmental Engineering, Ajou University, Suwon 16499, Republic of Korea*

[b]*Chemical & Process Technology Division, Korea Research Institute of Chemical Technology, Daejeon 34114, Republic of Korea. E-mail: hjkim@krict.re.kr*

[c]*School of Civil, Architectural Engineering, and Landscape Architecture & Department of Global Smart City, Sungkyunkwan University (SKKU), Suwon 16419, Republic of Korea. E-mail: jechanlee@skku.edu*

† Electronic supplementary information (ESI) available. See https://doi.org/10.1039/d2ta02060b

‡ Current affiliation: Department of Earth and Environmental Engineering, Columbia University, New York, NY 10027, USA.

Dr Jechan Lee received his PhD in chemical engineering from the University of Wisconsin–Madison in 2015 and M.S. in environmental engineering from Columbia University in 2010. After his PhD, he worked as a postdoctoral researcher at the Catalysis Center for Energy Innovation at the University of Delaware (2015–2016) and Sejong University (2016–2018). He was an assistant professor in the Department of Environmental and Safety Engineering (2018–2021) and as associate professor in the Department of Environmental and Safety Engineering/Department of Energy Systems research (2021–2022) at Ajou University. He has currently joined the faculty at Sungkyunkwan University (SKKU). His research interests are in the areas of waste upcycling, waste-to-energy, biorefinery, and CO_2 utilization. He has currently authored more than 210 peer-reviewed SCI(E) papers.

1. Introduction

Microplastics are a major problem in the fish-eat-fish world of sea and ocean environments. These prolific plastic particles are consumed by small fish, which are then eaten by larger fish, thereby transferring this pollutant up the food chain eventually to humans.[1] Microplastics originate from the colossal use of modern day plastics; these plastics deteriorate into smaller particles that may be consumed by marine fauna. Fishing nets are a major source of microplastics that has not previously been considered and are typically made of non-biodegradable nylon. Approximately 6.4×10^5 t of fishing nets were dumped, abandoned, or lost directly at sea, accounting for more than half the debris discarded in oceans.[2] The fishing net waste (FNW) often becomes entangled with each other and is almost impossible to separate. Entangled FNW not only poses a risk to marine mammals such as sea lions, large whales, and seals that may become entangled in the nets,[3] but they also block sunlight to plankton and algae, thereby disturbing primary production processes in marine ecosystems.[4] The management of FNW (*e.g.*, collecting and recycling) has recently emerged as a means to address this problem.[5]

Conventional disposal and recycling methods for FNW (*e.g.*, landfilling, mechanical methods, and incineration), are no longer sustainable. These methods are considered downcycling, which is characterized by inefficient heat energy recovery and yields lower-value products than the corresponding original commodities.[6] Recently, upcycling approaches that use waste as feedstock to produce renewable chemicals have gained considerable attention. Among different waste materials, plastic waste is an emerging feedstock to produce energy and high-value chemicals and to synthesize useful carbonaceous materials.[7–10]

The thermocatalytic plastic upcycling process involves the catalytic conversion of plastics to high-value chemicals (*e.g.*, monomers and intermediates), at high temperatures between 300 and 700 °C. This process is attractive because it addresses plastic pollution by sustainably producing potentially value-added products.[11] It has high potential for the establishment of thermocatalytic plastic upcycling; hence, they have certainly shown great promise.[12] For example, styrene (a monomer of polystyrene) has been successfully recovered from expanded polystyrene waste with yields of up to 62.9% in the presence of Al_2O_3-supported metal catalysts (*e.g.*, Zn/Al_2O_3 and Mg/Al_2O_3) at 450 °C.[13,14] Polyethylene terephthalate monomers have been recovered from abandoned beverage bottles *via* thermocatalytic glycolysis (with ethylene glycol),[15] or aminolysis (with ethanolamine)[16] in the presence of guanidine catalysts such as triazabicyclodecene. A $Pt/SrTiO_3$ catalyst prepared by atomic layer deposition was used to make linear hydrocarbons from disposable polyethylene bags *via* thermocatalytic hydrogenolysis.[17] Another study achieved a >99% yield of linear hydrocarbons at 300 °C under 1.2 MPa H_2 without any solvent; the non-catalytic thermal treatment of disposable polyethylene bags did not yield any linear hydrocarbons.[17]

Recently, CO_2 has been suggested as a reaction medium for the thermocatalytic conversion of plastic waste, as a strategy for CO_2 utilization. For instance, using CO_2 and a HZSM-11 catalyst to thermocatalytically treat teabag waste at 500 °C improved nylon monomer recovery compared to that using typical thermal treatment.[18] Jung *et al.* investigated the thermocatalytic production of H_2 from polymeric waste with a Ni/SiO_2 catalyst in a CO_2 environment.[19] They found that utilizing CO_2 enhanced H_2 production from waste fishing nets, reaching >1090 mmol g_{cat}^{-1} h^{-1}; this was nine fold higher than the production rate obtained without CO_2.[19]

The preparation of catalysts from waste materials is another waste-upcycling method. Utilizing waste materials to prepare

Fig. 1 Conceptual diagram of marine waste upcycling proposed in this study.

and use a catalyst to generate renewable target products from other waste materials creates an eco-friendlier and more cost effective waste upcycling process.[20–22] Seashell waste is a potential waste material that is highly abundant; it is generated worldwide and approximately 35–70 wt% of seashells become waste.[23] In China, approximately 10 million t of seashell waste are landfilled annually.[24] Although a small fraction of seashell waste is re-used for handicrafts and fertilizers, its re-use for such purposes is limited due to its cost ineffectiveness and environmental problems such as soil solidification.[25] Improperly treated seashell waste (*e.g.*, illegal dumping) pollutes reclaimed land and public water and generates foul odors.[26] The preparation of solid base catalysts from seashell waste has been widely investigated for transesterification reactions[27–30] and catalytic pyrolysis of polymeric waste.[31] However, no studies have been performed on the thermocatalytic upcycling of plastic waste using catalysts made from natural seashell waste under different atmospheres.

This study investigated the recovery of caprolactam from FNW *via* thermocatalytic conversion under a CO_2 atmosphere using seashell waste-derived catalysts (SSWCs); as such, this demonstrated a strategy to concurrently upcycle marine waste while utilizing CO_2. To the best of our knowledge, this is the first ever study on synergistical CO_2 utilization for waste valorization and catalytic material preparation. Fig. 1 schematically describes the concept of this study. Two different catalysts were prepared from seashell waste *via* thermal treatment under N_2 and CO_2 atmospheres, and their catalytic performances were compared to maximize CO_2 utilization during waste upcycling. This work aims to offer an environmentally friendly treatment and concomitant production of value-added products from marine waste. This proposed strategy will also contribute to solving regional/global environmental problems, such as microplastic pollution.

2. Materials and methods

2.1. Feedstocks and catalyst preparation

FNW and seashell waste were collected from a beach near Buan County, North Jeolla Province, Republic of Korea. Collected FNW was cut to a length of 20–25 mm (Fig. S1†), while collected seashell waste was thoroughly washed, dried in an oven at 60 °C for 24 h, and pulverized to fine powder between 0.15 and 0.6 mm. To prepare two different SSWCs, seashell waste powder (100 g) was first carbonized at 400 °C (2.5 °C min^{-1}) under flowing ultra-high purity (UHP) N_2 or CO_2 gas at 300 mL min^{-1} for 2 h. The resultant char was mixed with a 6 M potassium hydroxide (KOH) solution (1 : 3, w/w) and maintained at 60 °C for 24 h. Then, the material was heated to 400 °C at 10 °C min^{-1}, under flowing UHP N_2 or UHP CO_2 at 300 mL min^{-1} and maintained for 30 min. This was followed by heating to 700 °C at 3 °C min^{-1}, after which the sample was maintained for 1 h under flowing UHP N_2 or UHP CO_2 at 300 mL min^{-1}. The resultant catalyst was treated with a 2 M hydrochloric acid (HCl) solution at 90 °C for 1 h, followed by washing with deionized water. Finally, the sample was dried at 60 °C for 24 h. The samples prepared under N_2 and CO_2 atmospheres were denoted as SSWC-N_2 and SSWC-CO_2, respectively.

2.2. Feedstock characterization

FNW was analyzed with Fourier-transform infrared spectroscopy (FTIR) using a Nicolet iS50 FTIR spectrometer (Thermo Fisher Scientific; Waltham, MA, USA) to identify its chemical composition.

The American Society for Testing and Materials (ASTM) D6980-17, ASTM D1203-21, and ASTM D5630-94 standard test methods were used to determine the moisture, volatile matter, and ash content in FNW, respectively. The difference between the initial sample mass and the total moisture, volatile matter, and ash content was considered as the fixed matter content in FNW. The elemental composition of FNW was determined using a FlashSmart 2000 elemental analyzer (Thermo Fisher Scientific; Waltham, MA, USA). Thermogravimetric analysis (TGA) of a 30 mg sample of FNW, which was heated at 10 °C min^{-1}, was conducted using an STA449 F3 thermal analyzer (NETZSCH; Selb, Germany).

2.3. Catalyst characterization

The composition of the SSWC-N_2 and SSWC-CO_2 catalysts was determined using an inductively coupled plasma-optical emission spectrometer (ICP-OES; iCAP™ PRO XP DUO, Thermo Fisher Scientific; Waltham, MA, USA).

A JSM-7900F scanning electron microscope (SEM) (JEOL; Akishima, Tokyo, Japan) was used to characterize the morphology of the SSWC-N_2 and SSWC-CO_2 catalysts. X-ray diffraction (XRD) was conducted using an X-ray diffractometer (D/MAX-2200 Ultima, Rigaku Corp.; Tokyo, Japan); the XRD used Cu Kα radiation ($\lambda = 0.154$ nm) and operated at 40 kV and 40 mA. The crystalline phase of the sample was identified using the International Center for Diffraction Data database.

Physisorption measurements were performed using an ASAP 2020 system (Micromeritics; Norcross, GA, USA) using N_2 to assess the adsorption–desorption isotherms at −196 °C. Prior to measurement, the samples were degassed at 90 °C for 30 min, followed by heating at 150 °C for 12 h in a vacuum.

A temperature programmed desorption of NH_3 (NH_3-TPD) was performed to analyze surface acidity using an AutoChem II 2920 system (Micromeritics; Norcross, GA, USA). The samples were pretreated in the presence of He for 1 h at 500 °C and 0.5 h at 150 °C. Then, the samples were saturated with 15 vol% NH_3 in He. Changes in thermal conductivity detector (TCD) signals were recorded between 150 and 500 °C at a ramp rate of 5 °C min^{-1}, in which the samples were maintained for 1 h in the presence of flowing He at 50 mL min^{-1}.

Chemisorption measurements of samples were conducted using an ASAP2010 system (Micromeritics; Norcross, GA, USA), using 99.999 vol% CO_2 as analysis gas. The samples were pretreated with He for 2 h at 500 °C; then, they were evacuated for 1 h at 35 °C such that the pressure was below 0.67 kPa. Adsorption isotherms were recorded at 35 °C to measure the CO_2 uptake by the samples.

A sequence of temperature-programmed reduction of H_2 (H_2-TPR), temperature-programmed oxidation of O_2 (O_2-TPO), and a repeat of H_2-TPR was carried out to probe reducibility using an AutoChem II 2920 (Micromeritics; Norcross, GA, USA). The samples were pretreated in the presence of Ar at 500 °C for 1 h and then cooled to 50 °C. During H_2-TPR, changes in the TCD signal were recorded between 50 and 500 °C at a ramp rate of 10 °C min^{-1}, in which the samples were maintained for 1 h in the presence of 10 vol% H_2 in Ar at 50 mL min^{-1}. A liquid trap was maintained at −70 °C to remove moisture from the gas prior to entering the TCD. After the sample was cooled to 50 °C in the presence of Ar, O_2-TPO was conducted within 40–500 °C at a ramp rate of 10 °C min^{-1}, where the samples were maintained for 1 h in the presence of 5 vol% O_2/Ar at 50 mL min^{-1}. After cooling the samples to 50 °C in the presence of Ar, H_2-TPR was repeated.

2.4. Thermocatalytic conversion of FNW

Fig. S2† presents a schematic of the reactor setup used for the thermocatalytic conversion of FNW. For non-catalytic experiments, 1 g of FNW was loaded into the reactor, which was purged by flowing UHP N_2 or UHP CO_2 at 100 mL min^{-1} for 10 min at room temperature (~23 °C) to remove all oxygen within the reactor. Then, the FNW feedstock was heated to 500 °C at 10 °C min^{-1} under flowing N_2 or CO_2 (the same gas used for purging) at 100 mL min^{-1}; the feedstock was maintained at 500 °C for 1 min. For *in situ* thermocatalytic conversion, a FNW and catalyst mixture (FNW/catalyst = 20, mass basis) was loaded into the reactor (Fig. S2a†). For *ex situ* thermocatalytic conversion, a catalyst bed was established after the feedstock to allow vaporized species from the FNW migrate through the catalyst bed (Fig. S2b†). The subsequent steps in this process were the same as those performed during the non-catalytic experiments.

2.5. Product analysis

A fusion gas analyzer micro-gas chromatograph (Micro GC) system (INFICON; Bad Ragaz, Switzerland) (see Fig. S2†) was used to identify and quantify the non-condensable compounds (*i.e.*, gaseous products) created during the thermocatalytic conversion of FNW; this system was directly connected to the reactor outlet. Condensable compounds (*i.e.*, caprolactam and other liquid by-products) were collected in the condenser (Fig. S2†) and quantified using an 8890 GC equipped with a 5977B mass spectrometer (MS) (Agilent Technologies; Santa Clara, CA, USA). The sample analysis conditions that were applied to the Micro GC and GC-MS systems are detailed in Tables S1 and S2,† respectively. Condensable compounds were identified by comparing their GC-MS spectrograms with those present in the National Institute of Standards and Technology mass spectral library. Pure caprolactam (product no. C2204, Sigma Aldrich; St Louis, MO, USA) was used to confirm GC-MS peaks corresponding to caprolactam by matching the mass spectrum with the retention time. The actual amount of caprolactam was quantified with an external standard method using a GC equipped with a flame ionization detector; the calibration curve with this method is shown in Fig. S3.† The caprolactam yield was calculated using eqn (1):

$$\text{Caprolactam yield (wt\%)} = 100 \times \left(\frac{\text{mass of caprolactam identified}}{\text{mass of FNW feedstock}}\right) \quad (1)$$

3. Results and discussion

3.1. Feedstock characterization

To identify the major repeating units of FNW, FTIR was utilized to characterize the key functional groups of FNW. The resultant FTIR spectra are shown in Fig. 2a; the FNW sample exhibited various peaks that corresponded to the characteristic peaks of polyamide 6,[32] indicating the composition of FNW.

Proximate analysis of FNW showed that it is composed of 97.48 wt% volatile matter, 0.01 wt% fixed carbon, 2.01 wt% moisture, and 0.50 wt% ash. Ultimate analysis revealed that FNW was composed of 63.06 wt% carbon, 10.28 wt% hydrogen, 13.89 wt% oxygen, 12.27 wt% nitrogen, and 0.50 wt% ash; the composition of FNW is summarized in Fig. 2b.

Fig. 2c and d illustrate the apparent thermal decomposition patterns of FNW under N_2 and CO_2 atmospheres, respectively, as recorded by TGA. An approximate 2 wt% mass loss was observed from 100 to 350 °C, corresponding to moisture evaporation (Fig. 2c), while a distinct decomposition zone between 350 and 500 °C occurred during the thermal degradation of FNW. Approximately 98 wt% of FNW was decomposed within this zone, which was consistent with its volatile matter content (Fig. 2b). Approximately 1 wt% of FNW remained after TGA; this residual mass was consistent with its fixed carbon and ash content (Fig. 2b). The mass change (Fig. 2c) and mass degradation rate (Fig. 2d) of FNW under a N_2 environment were difficult to differentiate from those obtained under a CO_2 environment. This means that CO_2 had no apparent effect on the thermal degradation of FNW (*i.e.*, the overall loss of thermal mass from FNW); however, CO_2 may affect the chemical composition and yield of products derived from FNW.

3.2. Non-catalytic thermal conversion of FNW

Fig. 3a shows that the non-catalytic thermal conversion of FNW produces gas, caprolactam, and liquid; no solids remained as full thermal degradation was achieved at 500 °C (Fig. 2c and d). Gaseous products from non-catalytic thermal conversion were composed of non-condensable gases such as H_2, CO, CO_2, and C_1–C_4 hydrocarbons; liquid products included a mixture of by-products in addition to caprolactam. Fig. S4† shows a representative GC-MS chromatogram of the liquid products yielded from the thermocatalytic conversion of FNW at 500 °C. The liquid by-products identified were classified as azepines (7-butyl-3,4,5,6(2*H*)-tetrahydroazepine, (*E*)-*N*-(azepan-2-ylidene) octan-1-amine, and 1-(3,4,5,6-tetrahydro-2*H*-azepin-7-yl)-2-azepanone), imines (2-methyl-6-tridecyl-6-piperidene, (*Z*)-octadec-9-en-1-imine, and 3-(pyrrolidin-1-yl)propan-1-imine),

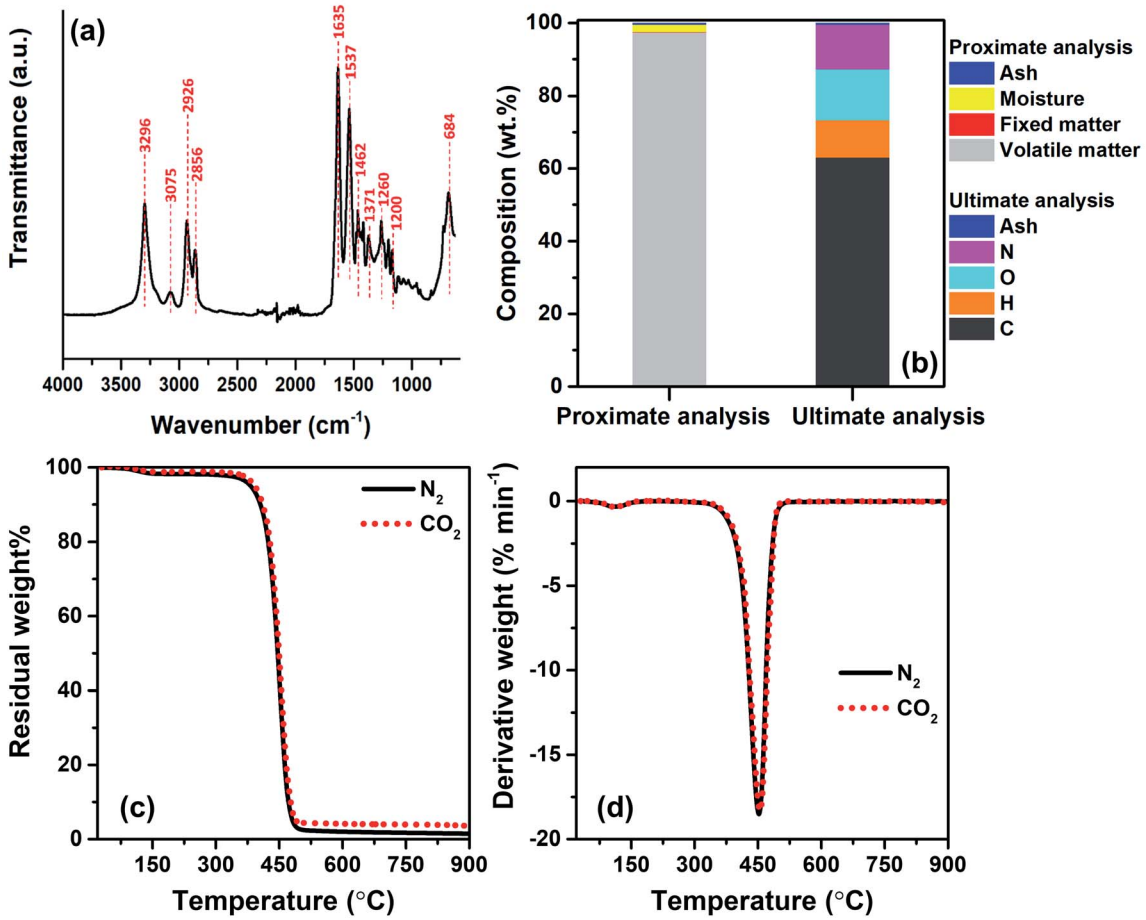

Fig. 2 (a) FTIR spectrum of FNW; (b) proximate and ultimate analyses results of FNW; (c) residual mass change in terms of temperature for the TGA of FNW under N_2 and CO_2 environments; and (d) derivative weight variation in terms of temperature for the TGA of FNW under N_2 and CO_2 environments.

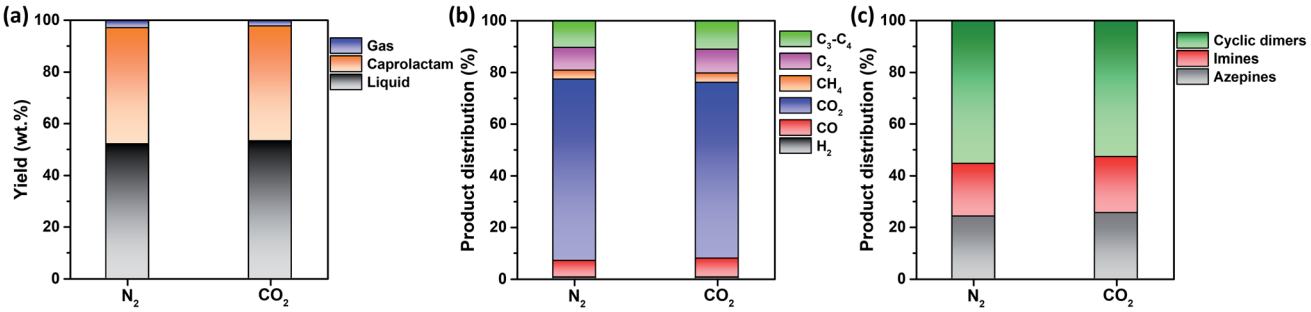

Fig. 3 (a) Yields of gaseous and liquid products, and caprolactam produced from the non-catalytic thermal conversion of FNW at 500 °C under N_2 and CO_2 environments; (b) distribution of gaseous products; (c) distribution of liquid products.

and cyclic dimers (1,8-diazacyclotetradecane-2,9-dione and 1,6,14-triazacyclohenicosane-2,7,15-trione) (see Table S3†).

In Fig. S5,† the change in the yield of caprolactam produced through the non-catalytic thermal conversion of FNW under N_2 and CO_2 atmospheres from 500 to 900 °C is presented. The caprolactam yield clearly decreased with increasing temperature from 500 to 900 °C. This is most likely due to thermal degradation of caprolactam itself at temperatures higher than 500 °C. The caprolactam yield obtained under N_2 and CO_2 was not significantly different at 500 and 600 °C; however, using the CO_2 medium in non-catalytic thermal conversion of FNW lowered the caprolactam yield at >600 °C (Fig. S5†). The use of CO_2 as a thermal conversion medium enhances the thermal cracking of volatile species evolved from feedstock (biomass or plastics),[33] which is favored at temperatures exceeding 700 °C.[34] This results in higher yields of gaseous products and lower

yields of liquid and solid products under a CO_2 atmosphere at >600 °C than those obtained using a typical inert medium such as N_2.[33] As such, at temperatures lower than 700 °C, the caprolactam yield achieved in N_2 and CO_2 was not significantly different. The temperature of 500 °C led to the highest caprolactam yield (Fig. S5†), and the full thermal degradation of FNW occurred at ~500 °C under both N_2 and CO_2 atmospheres (Fig. 2c and d). Therefore, 500 °C was used in further investigations on the thermocatalytic conversion of FNW.

Fig. 3a shows that the product yields obtained from the non-catalytic thermal conversion of FNW under N_2 and CO_2 atmospheres did not substantially differ. Enhanced thermal cracking of volatiles by CO_2 is favored at temperatures exceeding 700 °C;[34] as such, for the non-catalytic thermal conversion of FNW at 500 °C, CO_2 was an inert agent (*e.g.*, N_2). The distribution of gaseous and liquid products derived from FNW under a CO_2 atmosphere was similar to that under an N_2 atmosphere (Fig. 3b and c). The non-catalytic thermal conversion of FNW yielded approximately 45 wt% of caprolactam (Fig. 3a).

3.3. Catalyst characterization

The seashell waste used as the feedstock for the preparation of two SSWC catalysts was made mainly of polymorph of $CaCO_3$, such as aragonite, as proven by the XRD analysis (Fig. S6†). We prepared the SSWC-N_2 and SSWC-CO_2 catalysts *via* carbonization of seashell waste and sequential KOH-activation. Table 1 and Fig. 4 show the porosity of the SSWC catalysts through N_2-physisorption; both catalysts had low specific surface areas with type III isotherms, indicating low adsorbent–adsorbent interactions. SSWC-N_2 had a Brunauer, Emmett, and Teller specific surface area of 3.05 $m^2\ g^{-1}$; this was 1.82-fold higher than that of SSWC-CO_2. Both catalysts consist of bimodal pores, but the broad large peak above 10 nm indicates that the pores are irregular (Fig. 4). The low geometric surface areas indicate that the catalysts went through a molten state during the preparation to form the fused catalyst, mostly composed of surfaces.

Fig. 5a shows the SEM images of the SSWC-N_2 and SSWC-CO_2 catalysts. It is clearly shown that SSWC-CO_2 is more crystalline than SSWC-N_2, having a typical cubic shape morphology. As listed in Table S4,† the two catalysts were composed of various inorganic chemicals, with $CaCO_3$ being predominant. The carbonization of seashell waste under a CO_2 atmosphere increased the $CaCO_3$ content while decreasing the K content in the catalyst compared with that during carbonization under a N_2 atmosphere. The XRD patterns of SSWC-N_2 and SSWC-CO_2 are shown in Fig. 5b; the diffraction peaks of both catalysts were almost identical, representing $CaCO_3$ as per the ICDD database (JCPDS no. 01-072-1937), consistent with the ICP-OES results (Table S4†). This also indicates that a polymorphic transition of aragonite occurred during the carbonization of the seashell waste (Fig. S6† and 5b). Moreover, SSWC-CO_2 showed a higher XRD intensity than SSWC-N_2, indicating that the former has

Table 1 Physicochemical properties of SSWC-N_2[a] and SSWC-CO_2

	Surface area ($m^2\ g^{-1}$)		Pore volume ($cm^3\ g^{-1}$)				
Catalyst	BET	External[b]	Micropore[b]	Mesopore[c]	Total[d]	Average pore diameter[d] (nm)	Basicity[e] (mmol g^{-1})
SSWC-N_2	3.05	1.88	0.0005	0.1695	0.017	26.5	3.34
SSWC-CO_2	1.68	1.13	0.0002	0.0088	0.009	23.0	8.10

[a] Seashell waste-derived catalysts under N_2: SSWC-N_2, seashell waste-derived catalysts under CO_2: SSWC-CO_2, and BET: Brunauer, Emmett, and Teller. [b] Determined by the *t*-plot method. [c] Calculated by subtracting micropore volume from total pore volume. [d] Determined by the Barrett–Joyner–Halenda (BJH) desorption method at a relative pressure (P/P_0) of 0.99. [e] Measured using the CO_2 chemisorption method at a temperature of 35 °C.

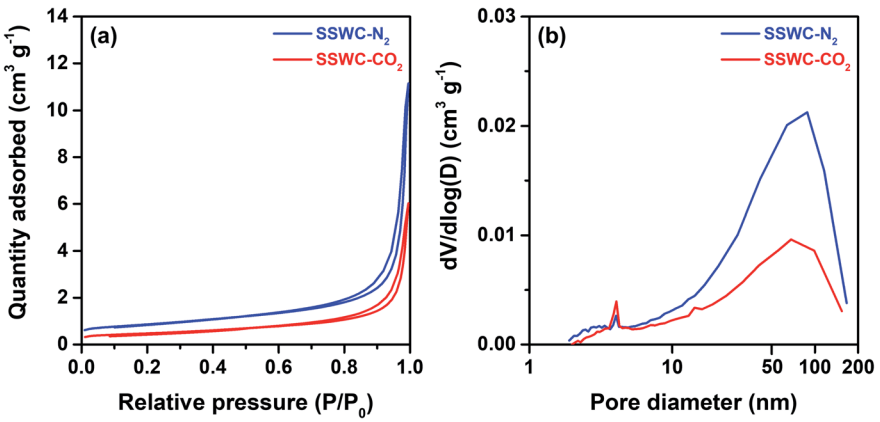

Fig. 4 (a) N_2 adsorption–desorption isotherm; (b) pore size distribution under N_2 physisorption for SSWC-N_2 and SSWC-CO_2.

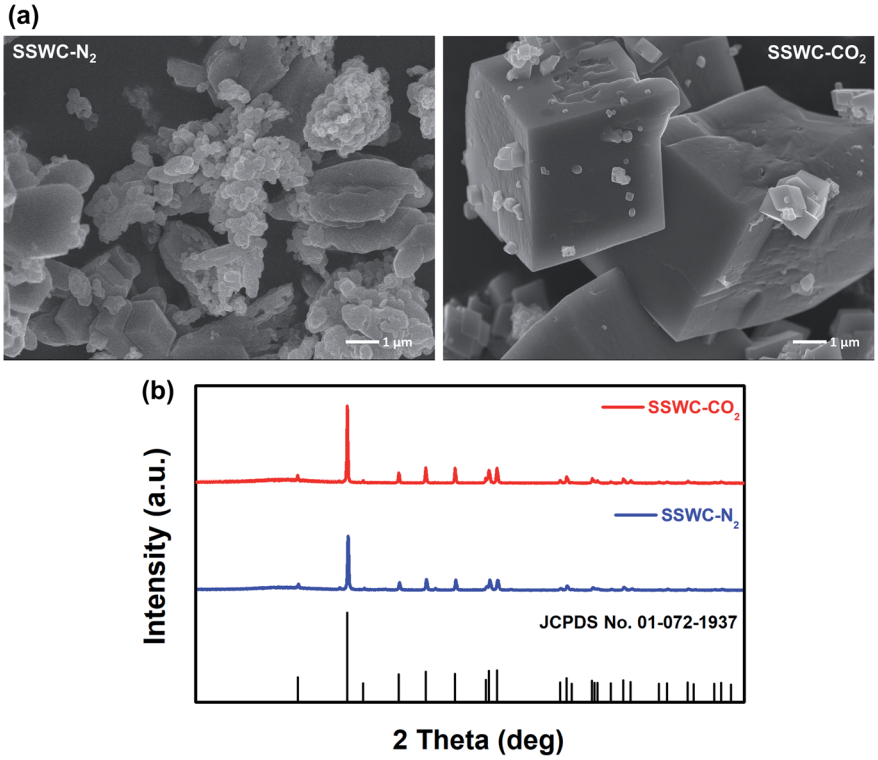

Fig. 5 (a) Scanning electron microscopy (SEM) images of SSWC-N_2 and SSWC-CO_2 (SEM images with a magnification of 5 μm are given in Fig. S7†); (b) XRD patterns of SSWC-N_2 and SSWC-CO_2.

a higher degree of crystallinity than the latter; these XRD results were supported by the SEM results (Fig. 5a).

Table 1 demonstrates that the increase in the $CaCO_3$ concentration of SSWC-CO_2 elevated CO_2 uptake, which was 2.43-fold higher than that of SSWC-N_2. Both catalysts exhibited negligible reducibility through the H_2-TPR/O_2-TPO/H_2-TPR sequence (Fig. S8†). This means that most impurities in SSWC, which occurred as various metals as shown in Table S4,† were not exposed to the surface. Similarly, nearly zero acid sites were observed on the surface of both catalysts as a result of NH_3-TPD (Fig. S9†). The characterization results indicate that the atmospheric variations, where seashell waste carbonization occurred (*e.g.*, N_2 or CO_2), may alter the physicochemical properties of the SSWC, affecting its basicity.

3.4. Thermocatalytic conversion of FNW using the SSWC catalysts

This study hypothesized that catalyst configuration during thermocatalytic processing may affect caprolactam recovery from FNW. Thus, two different catalyst loading configurations were tested: *in situ* and *ex situ*. For *in situ* configuration, the thermocatalytic conversion of FNW occurred within a reactor where FNW and the catalyst were mixed together to enable direct contact between the two (Fig. S2a†).[35,36] *Ex situ* configuration involved no direct contact between FNW and the catalyst; here, nets were first thermally cracked to release high molecular weight volatile species. Then, volatile species were passed through a catalyst bed in which they were further transformed into lower molecular weight species (Fig. S2b†).[35,36]

Fig. 6a shows yields for gaseous and liquid products, and caprolactam obtained *via* the thermocatalytic conversion of FNW under a N_2 atmosphere with and without the SSWC-N_2 catalyst, using *in situ* and *ex situ* configurations. The *ex situ* configuration did not significantly affect the caprolactam yield compared with that of the non-catalytic process; however, it increased the gaseous product yield while decreasing the liquid product yield compared with those from non-catalytic thermal conversion. This indicates that the catalyst improved the thermal cracking of high molecular weight volatiles released from FNW *via* thermal degradation. The use of the SSWC-N_2 catalyst in the *in situ* configuration increased the caprolactam yield to 63.6 wt%; thus, the thermal depolymerization of FNW to caprolactam was more selective using the *in situ* configuration than that using *ex situ* configuration. This may be attributed to the intimate contact of the catalyst with high molecular weight volatile species generated *via* thermal depolymerization.[37,38] The high diffusion efficiency of polymer-derived (*e.g.*, FNW-derived) heavy volatiles enables their diffusion into catalyst pores; this facilitates direct contact between volatiles and catalytic sites using *in situ* configuration.[39,40] This may amplify the catalytic effect for promoting the thermal depolymerization of FNW, which may potentially contribute to higher caprolactam yields than those derived from using *ex situ* configuration. The distributions of gaseous and liquid products in the three cases were similar (Fig. 6b and c). As the *in situ* configuration yielded the highest quantity of caprolactam, further experiments were conducted using this configuration.

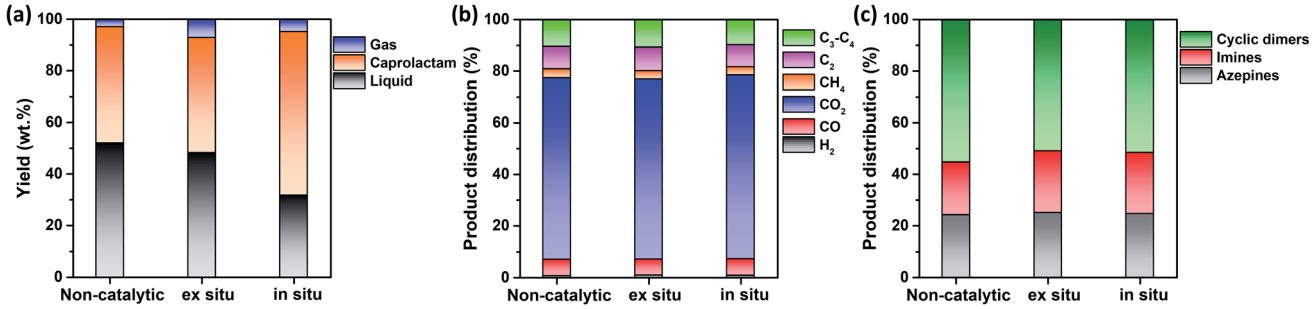

Fig. 6 (a) Yields of gaseous and liquid products, and caprolactam produced from the thermocatalytic conversion of FNW at 500 °C under an N_2 environment using SSWC-N_2 in different catalyst configurations; (b) distribution of gaseous products; (c) distribution of liquid products.

The base-catalyzed decomposition of polyamide 6 proceeds through an anionic chain mechanism, which occurs more rapidly than non-catalytic decomposition.[41] As shown in Fig. 7, this mechanism involves the base-catalyzed deprotonation of amide groups and the cleavage of the amide link that occurs on the polyamide 6 chain, followed by intramolecular cyclization that produces lactam units (*i.e.*, caprolactam). As the FNW feedstock used in this study is largely made up of polyamide 6 (Fig. 2a), the thermocatalytic conversion of these nets into caprolactam may follow a similar pathway.

Fig. 8 shows that the SSWC-CO_2 catalyst yields more caprolactam than the SSWC-N_2 catalyst under both N_2 and CO_2 atmospheres. For example, under an N_2 environment, the SSWC-CO_2 catalyst yielded more caprolactam (70.3 wt%) than the SSWC-N_2 catalyst (63.6 wt%). It is likely that this higher yield using the SSWC-CO_2 catalyst was due to the higher basicity of this catalyst compared with that of the SSWC-N_2 catalyst (Table 1). The use of CO_2 as a thermal conversion medium further enhanced the effectiveness of the SSWC catalyst in yielding caprolactam from FNW; for example, the yield reached 80 wt%

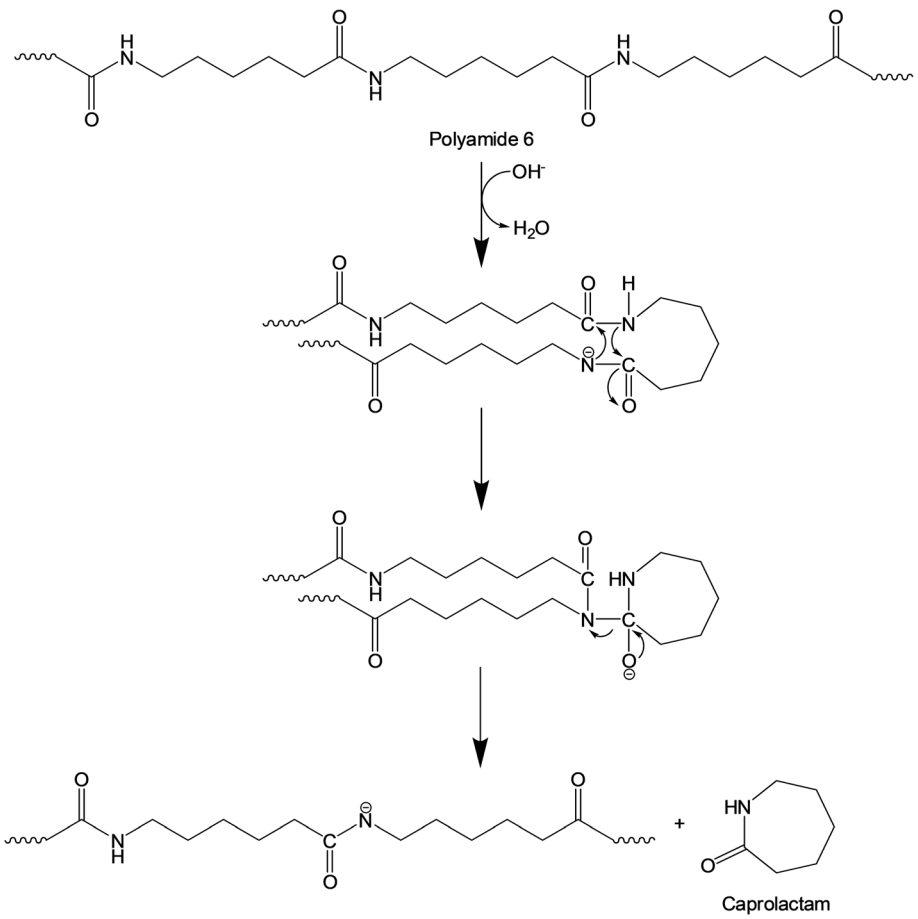

Fig. 7 Anionic chain reaction occurring in thermal degradation of polyamide 6 in the presence of a base catalyst.

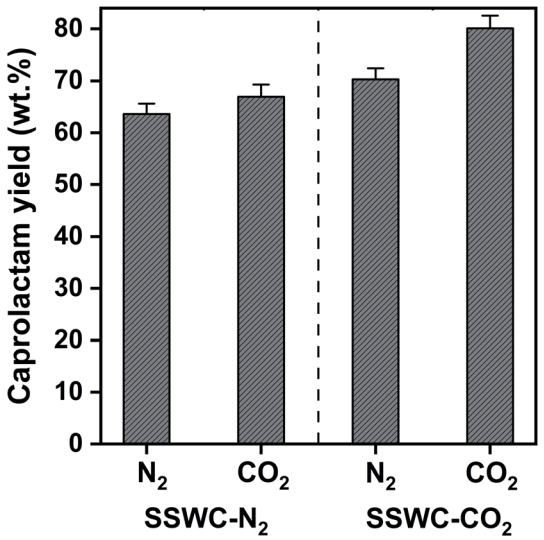

Fig. 8 Caprolactam yield from the thermocatalytic conversion of FNW at 500 °C under N_2 and CO_2 environments using SSWC-N_2 and SSWC-CO_2 in an *in situ* catalyst configuration.

when using the SSWC-CO_2 catalyst under a CO_2 environment. CO_2 molecules have been observed to interact with polar functional groups, modifying their reactivity on the catalyst surface.[42,43] Thus, the synergistic effect of the CO_2 reaction environment and the SSWC catalyst is most likely because the molecular interaction between CO_2 and the polar functional groups of FNW (*e.g.*, amides) causes the more reactive base-catalyzed deprotonation of amide groups and the cleavage of amide linkages.

Although there have been a limited number of literature reports, our results are compared with the most recent studies on thermocatalytic treatment of commercial nylon 6 and the feedstock similar to FNW, as summarized in Table S5.† The study done by Eimontas *et al.* has claimed 83% caprolactam yield (based on GC-MS area% without further quantification) with a ZSM-5 zeolite catalyst,[44] but the GC-MS area %-based yield cannot reflect the actual caprolactam yield. In another recent study that quantified the caprolactam yield using an external standard method (a similar method to ours), 70 wt% caprolactam yield was obtained from commercial nylon 6 with a scallop shell catalyst calcined under air.[31] In comparison, our yield (80 wt%; corresponding to ~91 GC-MS area %, as shown in Fig. S4†) is the highest among those that have been reported.

To assess the reusability of the SSWC-CO_2 catalyst, the spent SSWC-CO_2 catalyst was reused at 500 °C under a CO_2 atmosphere for three cycles; the results are shown in Fig. 9. A slight loss in the caprolactam yield was observed after each cycle. This is most likely due to coke deposition on the catalyst surface, as indicated by TGA analysis of the spent catalyst in air (Fig. S10†). The peaks ranging from 400 to 800 °C were attributed to the oxidation of coke.[45] In Fig. S10b,† the coke oxidation peak moved to higher temperature with increasing the number of reuse cycles, which indicates that harder oxidized coke was formed. Fig. S11† shows a SEM image of the spent SSWC-CO_2 catalyst after the 3rd reuse. In addition, the XRD patterns of fresh and spent catalysts are compared in Fig. S12.† The fresh catalysts exhibited higher XRD intensities than the spent catalysts, indicating that the spent ones have a lower degree of crystallinity than the fresh ones. Despite the yield loss, there was no significant reduction in the caprolactam yield as per the Student's *t*-test at the 95% confidence limit. Fig. 9 also shows that an increase in the SSWC-CO_2 catalyst loading did not influence the caprolactam yield; this demonstrates that the catalyst is reusable at an elevated catalyst loading.

Fig. 10 describes the marine waste upcycling process proposed in this study. As previously discussed, the thermocatalytic processing of FNW using the SSWC-CO_2 catalyst produced gases including CO_2, combustible gases (*e.g.*, H_2, CO, and C_1–C_4 hydrocarbons), and caprolactam-rich liquid products. Gaseous products were fed into a CO_2 separation system (*e.g.*, a monoethanolamine-based CO_2 capture process[46]); the separated CO_2 was recycled into the thermocatalytic FNW treatment or seashell waste carbonization. Combustible gases may be used as fuel to produce the heat and power required for thermocatalytic treatment and catalyst preparation. Caprolactam (80% wt yield based on the feedstock) was separated

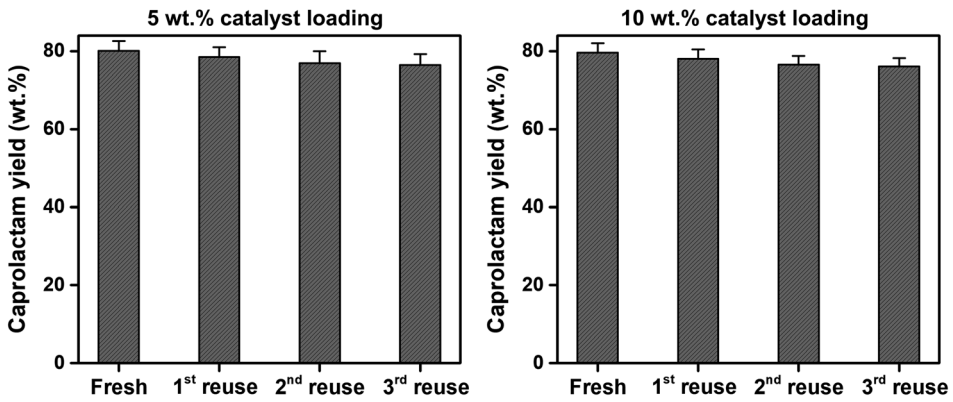

Fig. 9 Reusability of the spent SSWC-CO_2 catalyst with different catalyst loadings for the thermocatalytic conversion of FNW at 500 °C under a CO_2 environment.

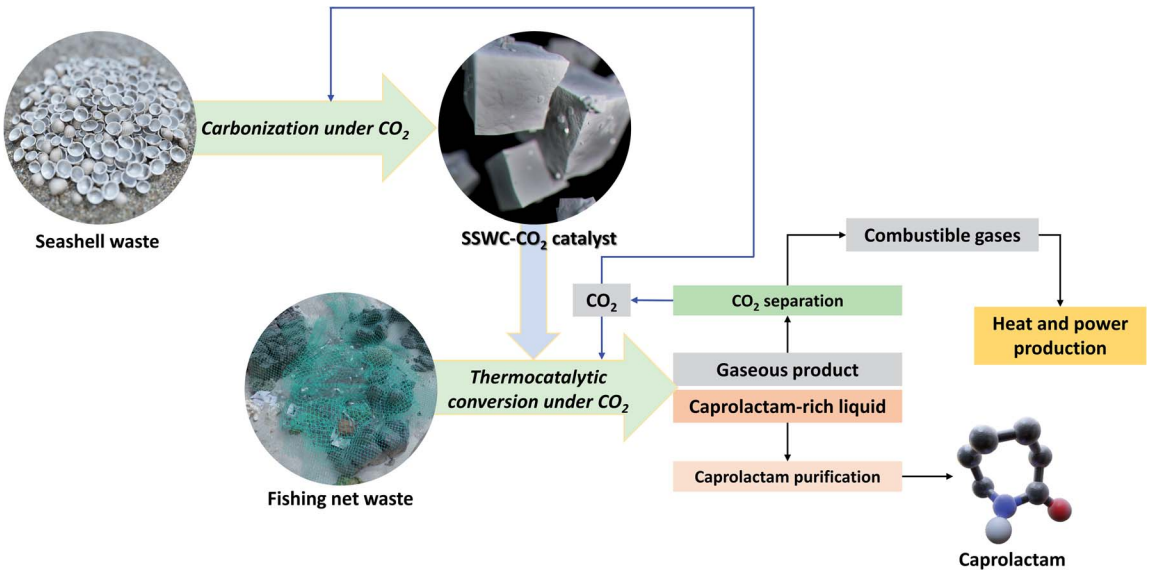

Fig. 10 Concept underpinning the thermocatalytic upcycling of marine waste (FNW and seashell waste) to monomer (caprolactam) under a CO_2 environment with the recycling of by-products.

from the caprolactam-rich liquid product *via* caprolactam purification using toluene or acetone as a solvent, and introducing a CO_2 flow.[47] This entire process potentially helps develop an energy-independent marine waste upcycling system that effectively utilizes CO_2.[48]

Globally, 640 000 t of fishing nets are abandoned in oceans every year,[5] contributing to the release of 7.1×10^{15} microplastic pieces (this estimate is based on data in Table S6†).[49] The thermocatalytic process depicted in Fig. 10 is able to convert 80% wt of FNW into caprolactam, valued at roughly one billion USD (Table S6†). This implies that the proposed marine waste upcycling process may potentially realize the reduction of microplastic pollution and increase the economic potential for marine waste valorization, such as with FNW and seashell waste.

4. Conclusions

This study performed the thermocatalytic treatment of FNW with catalysts prepared by carbonizing seashell waste under N_2 and CO_2 atmospheres (SSWC-N_2 and SSWC-CO_2, respectively). This method reclaimed value from different marine waste materials (*e.g.*, FNW and seashell waste) simultaneously. FNW used as feedstock in this study was made of polyamide 6, as confirmed by FTIR analysis. The carbonization environment materially affected the properties of the catalyst, such as its $CaCO_3$ content and basicity. The SSWC-CO_2 catalyst had a higher basicity and $CaCO_3$ content than SSWC-N_2. The SSWC catalysts enhanced the caprolactam yield (a value-added chemical used as the monomer of nylon 6), compared with the non-catalytic thermal conversion of FNW because the selective depolymerization of the polyamide bond to caprolactam involved base-catalyzed reactions. For the thermocatalytic conversion of FNW using a SSWC catalyst, the *in situ* catalyst configuration provided a higher caprolactam yield than that from the *ex situ* configuration. Base-catalyzed caprolactam production using the SSWC-CO_2 catalyst (*in situ* configuration) was further promoted in the thermocatalytic conversion of FNW carried out under a CO_2 atmosphere; the caprolactam yield reached 80 wt% of the FNW feedstock (a higher reported yield than previous studies), and the SSWC-CO_2 catalyst was stable after three consecutive cycles. There is no single simple solution for concurrently achieving marine waste upcycling with CO_2 utilization. Although this industry is still in its infancy, continuous research and development should help advance this industry to become economically viable.

Conflicts of interest

There are no conflicts to declare.

Acknowledgements

This work was supported by the National Research Foundation of Korea (NRF) grant funded by the Government of Republic of Korea (Ministry of Science and ICT) (No. 2020R1C1C1003225).

References

1 D. Kindy, *With Ropes and Nets, Fishing Fleets Contribute Significantly to Microplastic Pollution*, Smithsonian Magazine, 2021.
2 Sea Around Us, **https://www.seaaroundus.org**, accessed January 13, 2022.
3 One Green Planet, **https://www.onegreenplanet.org**, accessed January 13, 2022.
4 S. Orasutthikul, D. Unno and H. Yokota, *Constr. Build. Mater.*, 2017, **146**, 594–602.
5 M. Charter, R. Carruthers and S. F. Jensen, *Products from Waste Fishing Nets*, Circular Ocean led by the Environmental Research Institute, Scotland, 2018.
6 A. Rahimi and J. M. García, *Nat. Rev. Chem.*, 2017, **1**, 0046.

7 J. Gong, X. Chen and T. Tang, *Prog. Polym. Sci.*, 2019, **94**, 1–32.
8 B. Zhang, C. Song, C. Liu, J. Min, J. Azadmanjiri, Y. Ni, R. Niu, J. Gong, Q. Zhao and T. Tang, *J. Mater. Chem. A*, 2019, **7**, 22912–22923.
9 N. Liu, Z. Hu, L. Hao, H. Bai, P. He, R. Niu and J. Gong, *J. Environ. Chem. Eng.*, 2022, **10**, 106959.
10 F. Zhang, F. Wang, X. Wei, Y. Yang, S. Xu, D. Deng and Y.-Z. Wang, *J. Energy Chem.*, 2022, **69**, 369–388.
11 L. O. Mark, M. C. Cendejas and I. Hermans, *ChemSusChem*, 2020, **13**, 5808–5836.
12 J. Lee, E. E. Kwon, S. S. Lam, W.-H. Chen, J. Rinklebe and Y.-K. Park, *J. Cleaner Prod.*, 2021, **321**, 128989.
13 J. Shah, M. R. Jan and Adnan, *J. Ind. Eng. Chem.*, 2014, **20**, 3604–3611.
14 J. Shah, M. R. Jan and Adnan, *J. Anal. Appl. Pyrolysis*, 2015, **114**, 163–171.
15 K. Fukushima, O. Coulembier, J. M. Lecuyer, H. A. Almegren, A. M. Alabdulrahman, F. D. Alsewailem, M. A. Mcneil, P. Dubois, R. M. Waymouth, H. W. Horn, J. E. Rice and J. L. Hedrick, *J. Polym. Sci., Part A: Polym. Chem.*, 2011, **49**, 1273–1281.
16 K. Fukushima, J. M. Lecuyer, D. S. Wei, H. W. Horn, G. O. Jones, H. A. Al-Megren, A. M. Alabdulrahman, F. D. Alsewailem, M. A. McNeil, J. E. Rice and J. L. Hedrick, *Polym. Chem.*, 2013, **4**, 1610–1616.
17 G. Celik, R. M. Kennedy, R. A. Hackler, M. Ferrandon, A. Tennakoon, S. Patnaik, A. M. LaPointe, S. C. Ammal, A. Heyden, F. A. Perras, M. Pruski, S. L. Scott, K. R. Poeppelmeier, A. D. Sadow and M. Delferro, *ACS Cent. Sci.*, 2019, **5**, 1795–1803.
18 S. Kim, N. Lee, S. W. Lee, Y. T. Kim and J. Lee, *Chem. Eng. J.*, 2021, **412**, 128626.
19 S. Jung, D. Choi, Y.-K. Park, Y. F. Tsang, N. B. Klinghoffer, K.-H. Kim and E. E. Kwon, *Chem. Eng. J.*, 2020, **399**, 125889.
20 J. Gong, J. Liu, X. Chen, Z. Jiang, X. Wen, E. Mijowska and T. Tang, *J. Mater. Chem. A*, 2015, **3**, 341–351.
21 J. A. Bennett, K. Wilson and A. F. Lee, *J. Mater. Chem. A*, 2016, **4**, 3617–3637.
22 D. Li, W. Chen, J. Wu, C. Q. Jia and X. Jiang, *J. Mater. Chem. A*, 2020, **8**, 24977–24995.
23 Z. Yao, M. Xia, H. Li, T. Chen, Y. Ye and H. Zheng, *Crit. Rev. Environ. Sci. Technol.*, 2014, **44**, 2502–2530.
24 K. H. Mo, U. J. Alengaram, M. Z. Jumaat, S. C. Lee, W. I. Goh and C. W. Yuen, *Constr. Build. Mater.*, 2018, **162**, 751–764.
25 E.-I. Yang, S.-T. Yi and Y.-M. Leem, *Cem. Concr. Res.*, 2005, **35**, 2175–2182.
26 G.-L. Yoon, B.-T. Kim, B.-O. Kim and S.-H. Han, *Waste Manag.*, 2003, **23**, 825–834.
27 N. Viriya-empikul, P. Krasae, B. Puttasawat, B. Yoosuk, N. Chollacoop and K. Faungnawakij, *Bioresour. Technol.*, 2010, **101**, 3765–3767.
28 S. Hu, Y. Wang and H. Han, *Biomass Bioenergy*, 2011, **35**, 3627–3635.
29 W. Jindapon, S. Jaiyen and C. Ngamcharussrivichai, *Energy Convers. Manage.*, 2016, **122**, 535–543.
30 A. Perea, T. Kelly and Y. Hangun-Balkir, *Green Chem. Lett. Rev.*, 2016, **9**, 27–32.
31 N. Chaihad, I. Kurnia, A. Yoshida, C. Watanabe, K. Tei, P. Reubroycharoen, Y. Kasai, A. Abudula and G. Guan, *J. Anal. Appl. Pyrolysis*, 2020, **146**, 104750.
32 K.-H. Lee, K.-W. Kim, A. Pesapane, H.-Y. Kim and J. F. Rabolt, *Macromolecules*, 2008, **41**, 1494–1498.
33 N. Lee, S. Kim and J. Lee, *J. CO2 Util.*, 2021, **44**, 101414.
34 C. Park, S. Lee and J. Lee, *Chem. Eng. J.*, 2022, **427**, 131459.
35 A. Corma, S. Iborra and A. Velty, *Chem. Rev.*, 2007, **107**, 2411–2502.
36 E. Butler, G. Devlin, D. Meier and K. McDonnell, *Renewable Sustainable Energy Rev.*, 2011, **15**, 4171–4186.
37 K. Wang, P. A. Johnston and R. C. Brown, *Bioresour. Technol.*, 2014, **173**, 124–131.
38 Y. Shirazi, S. Viamajala and S. Varanasi, *Front. Chem.*, 2020, **8**, 786.
39 Y.-K. Park, J. S. Jung, J. Jae, S. B. Hong, A. Watanabe and Y.-M. Kim, *Chem. Eng. J.*, 2019, **377**, 119742.
40 H. Shafaghat, H. W. Lee, Y. F. Tsang, D. Oh, J. Jae, S.-C. Jung, C. H. Ko, S. S. Lam and Y.-K. Park, *Chem. Eng. J.*, 2019, **366**, 330–338.
41 H. Bockhorn, A. Hornung, U. Hornung and J. Weichmann, *Thermochim. Acta*, 1999, **337**, 97–110.
42 S.-i. Fujita, Y. Onodera, H. Yoshida and M. Arai, *Green Chem.*, 2016, **18**, 4934–4940.
43 C. Park and J. Lee, *Green Chem.*, 2020, **22**, 2628–2642.
44 J. Eimontas, S. Yousef, N. Striūgas and M. A. Abdelnaby, *Renewable Energy*, 2021, **179**, 1385–1403.
45 H. Zhang, Y. Wang, S. Shao and R. Xiao, *Sci. Rep.*, 2016, **6**, 37513.
46 K. Li, A. Cousins, H. Yu, P. Feron, M. Tade, W. Luo and J. Chen, *Energy Sci. Eng.*, 2016, **4**, 23–39.
47 L. Moens, *US Pat.*, US5919927A, 1999.
48 S. Kim, J. Byun, H. Park, N. Lee, J. Han and J. Lee, *Energy*, 2022, **241**, 122876.
49 L. S. Wright, I. E. Napper and R. C. Thompson, *Mar. Pollut. Bull.*, 2021, **173**, 113115.

